Electron-phonon heat transfer in monolayer and bilayer graphene

J. K. Viljas and T. T. Heikkilä

Low Temperature Laboratory, Aalto University, P.O. Box 15100, FI-00076 AALTO, Finland
(Received 17 February 2010; revised manuscript received 26 April 2010; published 1 June 2010)

We calculate the heat transfer between electrons to acoustic and optical phonons in monolayer and bilayer graphene (MLG and BLG) within the quasiequilibrium approximation. For acoustic phonons, we show how the temperature-power laws of the electron-phonon heat current for BLG differ from those previously derived for MLG and note that the high-temperature (neutral-regime) power laws for MLG and BLG are also different, with a weaker dependence on the electronic temperature in the latter. In the general case we evaluate the heat current numerically. We suggest that a measurement of the heat current could be used for an experimental determination of the electron-acoustic-phonon coupling constants, which are not accurately known. However, in a typical experiment heat dissipation by electrons at very low temperatures is dominated by diffusion and we estimate the crossover temperature at which acoustic-phonon coupling takes over in a sample with Joule heating. At even higher temperatures optical phonons begin to dominate. We study some examples of potentially relevant types of optical modes, including, in particular, the intrinsic in-plane modes and additionally the remote surface phonons of a possible dielectric substrate.

I. INTRODUCTION

In the presence of Joule heating, the static temperature of the conduction electrons of a metallic system is set by the heat balance between the heating and energy relaxation. The latter is caused either by electron diffusion away from the heated region or by the energy transfer to the lattice via the electron-phonon coupling. If the lattice can transfer its energy effectively enough to the underlying substrate, a hot-electron situation may be reached, where the electronic temperature T_e is considerably higher than that of the (acoustic) phonons, T_{ac}.[1–3] More generally, such a situation with well-defined separate electron and phonon temperatures is known as quasiequilibrium. In analyzing experiments or devices that involve heating (or cooling[4]) effects of this kind, it is essential to be able to model the heat currents between the various subsystems.[3] This is particularly important in two-dimensional (2D) graphene, which has a small thermal volume and is thus easily overheated. Of central interest here is the heat current between the electrons and the phonons, on which we concentrate in this paper.

In metals at sufficiently low temperatures only acoustic phonons are relevant and of those the longitudinal-acoustic (LA) modes have the strongest coupling constants. At very low temperature the power transferred between the electrons and LA phonons (assuming quasiequilibrium) is typically of the form

$$Q_{e\text{-}ac} = V_d \Sigma (T_e^\delta - T_{ac}^\delta), \qquad (1)$$

where V_d is the d-dimensional volume and Σ is a coupling constant. This form is well known in the case of simple three-dimensional (3D) metals, where the exponent is $\delta=5$ (Refs. 2 and 5). In lower-dimensional and disordered systems different exponents have been found. In disordered thin films $\delta=6$ has been observed[6,7] and in thin doubly clamped metallic beam, where the electrons remain 3D but vibrations are one dimensional, $\delta=3$ and V_d is the length of the beam.[4]

The electron cooling power and temperature relaxation times were recently studied theoretically also for monolayer graphene (MLG).[8–10] Graphene is a single sheet of graphite, i.e., a 2D honeycomb lattice of carbon, which has (semi)metallic properties.[11,12] In its monolayer form the valence (v) and conduction (c) bands touch at the two K points of the Brillouin zone (or Dirac points), around which the electron dispersion relation is conical. In bilayer graphene (BLG) the dispersion is approximately parabolic.[13] The most important difference of graphene to other metals or semiconductors is the "chiral" character of the charge carriers. However, close to the charge neutrality point the properties of graphene differ from other metals already by the special forms of the dispersion relations. In Ref. 8 it was found that at low temperature the power transferred to in-plane LA phonons in MLG is of the usual form (1) with $\delta=4$ [see Eq. (15) below]. In Ref. 9, on the other hand, it was shown that in the neutral (or high-temperature) regime of MLG the power has a form asymmetric in T_e and T_{ac},

$$Q_{e\text{-}ac} = V_d g(\mu, T_e)(T_e - T_{ac}), \qquad (2)$$

where $V_d=A$, the area of the sample, $g(\mu, T_e)$ is a function which we specify in Eq. (17) below, and μ the chemical potential measured from the Dirac point.

In this paper we revisit the problem of electron-phonon power transfer in MLG and consider also the case of BLG in the parabolic-band approximation. We show that the conditions for the validity of the "low-temperature" and "high-temperature" results for MLG mentioned above are roughly $T_e, T_{ac} \ll T_{\text{BG,MLG}}$ and $T_e, T_{ac} \gg T_{\text{BG,MLG}}$, respectively, where $T_{\text{BG,MLG}}=2(c/v)|\mu|/k_B$ is the Bloch-Grüneisen (BG) temperature of MLG. Here $v \approx 1 \times 10^6$ m/s is the Fermi speed in MLG and $c \approx 2 \times 10^4$ m/s $\ll v$ is the speed of sound. These two limits have been termed the BG and equipartition (EP) regimes, respectively.[14] In these limits we recover the previously derived results [Eqs. (15) and (17)] but in addition to studying the limits analytically, we evaluate the power numerically in the crossover region. We then repeat the same

analysis for BLG, where $T_{\text{BG,BLG}}=2(c/v)\sqrt{\gamma_l|\mu|}/k_B$, with γ_l the interlayer coupling amplitude. Also for BLG, in the BG regime the usual power-law form (1) for acoustic phonons is found, with $\delta=4$, while the result in the opposite regime has form (2) [Eqs. (19) and (21)]. In fact the exponent $\delta=4$ is independent of the chirality of the carriers since it appears that in nondisordered systems at low temperatures quite generally $\delta=d+2$, where d is the smaller of the dimensions of the electron and the phonon systems. However, the coupling constants Σ for MLG and BLG depend rather differently on doping, with $\Sigma\propto|\mu|$ in MLG and $\Sigma\propto 1/\sqrt{|\mu|}$ in BLG. These differences in Σ can be understood based on the electron-phonon relaxation rates and electronic specific heats. In the EP regime we find that the temperature dependence of $g(\mu,T_e)$ is weaker in BLG ($g\sim T_e$) than in MLG ($g\sim T_e^4$).

At very low temperatures the most efficient energy relaxation mechanism for electrons is diffusion. In order to measure $Q_{e\text{-}ac}$ for determining the coupling constant Σ, the temperature should be higher than a certain value which we estimate in Sec. VII for a typical experimental situation. On the other hand, at even higher temperatures the optical-phonon power becomes dominant. To estimate also the temperature for this crossover, we consider some simplified models for optical phonons that may be relevant. The most obvious ones are the intrinsic in-plane longitudinal-optical (LO) or transverse-optical (TO) modes. For graphene on a dielectric substrate, the surface optical phonons of the dielectric must also be considered.[15,16] We find that the latter can begin to dominate the energy relaxation already at much lower temperatures than the intrinsic phonons.

In suspended graphene, in addition to the LA phonons, also out-of-plane acoustic (flexural) modes should be considered.[17] However, these are disregarded here as their coupling to electrons is only of second order in the displacements and since they should not be important for graphene on a substrate. On the other hand, we also do not discuss explicitly the coupling of the graphene phonons to those of the substrate or the heat transfer (Kapitza resistance) between them,[18] which, although an important part of the heat-balance problem, depends on the details of the interface and is difficult to model microscopically. This coupling may to some extent affect the acoustic-phonon dispersions and the relevant LA phonons should possibly be understood as collective surface acoustic modes of the coupled graphene-substrate system. Finally, we do not take into account effects of impurities or discuss explicitly electron-electron interactions, which are assumed to be strong enough to keep the electrons in quasiequilibrium.

This paper is organized as follows. In Sec. II we sketch our Boltzmann golden-rule approach for calculating the heat current and briefly discuss the quasiequilibrium approximation. Next we give a brief reminder on the low-energy electronic structure of graphene in Sec. III and then continue to consider the coupling of the electrons to LA phonons via a deformation-potential approach in Secs. IV and V. In Sec. VI, we describe our models for the optical phonons and their coupling to electrons, and the calculation of the corresponding heat currents. Finally, we discuss the experimental consequences of our results and the crossover temperatures in Sec. VII.

II. ELECTRON-PHONON HEAT TRANSFER FROM THE BOLTZMANN THEORY AND FERMI GOLDEN RULE

Below we derive a general expression for the electron-phonon heat current by employing a Boltzmann collision integral in the Fermi golden rule approximation. In what follows, we disregard the spin and valley indices, which only appear as an additional degeneracy factor $g_e=4$ in the results.

The position-independent Boltzmann equation describing the occupation probability f_k^α of the electron excitation with momentum $\hbar k$ in band α is

$$\partial_t f_k^\alpha = S_{e\text{-}ph}(f_k^\alpha). \tag{3}$$

Here the collision integral is given by

$$S_{e\text{-}ph}(f_k^\alpha) = -\sum_{p\beta}[f_k^\alpha(1-f_p^\beta)W_{k\alpha\to p\beta} - f_p^\beta(1-f_k^\alpha)W_{p\beta\to k\alpha}], \tag{4}$$

where the golden-rule scattering rates are

$$W_{k\alpha\to p\beta} = \frac{2\pi}{\hbar}\sum_{q\gamma} w_{kp,q}^{\alpha\beta,\gamma}[(n_q^\gamma+1)\delta_{k,p+q}\delta(\epsilon_{kp}^{\alpha\beta}-\omega_q^\gamma)$$
$$+ n_q^\gamma\delta_{k,p-q}\delta(\epsilon_{kp}^{\alpha\beta}+\omega_q^\gamma)]. \tag{5}$$

In these n_q^γ is the distribution function of phonons with momentum $\hbar q$ and band index γ, ϵ_k^α and ω_q^γ are the electron and phonon excitation energies, and we defined $\epsilon_{kp}^{\alpha\beta}=\epsilon_k^\alpha-\epsilon_p^\beta$. We assume the electron-phonon coupling constants to satisfy the symmetries $w_{kp,q}^{\alpha\beta,\gamma}=w_{pk,q}^{\beta\alpha,\gamma}=w_{kp,-q}^{\alpha\beta,\gamma}$. The power with which the phonons cool the electrons (i.e., the electron-phonon heat current) is defined by

$$Q = -\partial_t\sum_{k\alpha}\epsilon_k^\alpha f_k^\alpha = -\sum_{k\alpha}\epsilon_k^\alpha S_{e\text{-}ph}(f_k^\alpha). \tag{6}$$

It is convenient to divide the power into two terms according to whether they describe induced (stimulated) or spontaneous processes.[2] Thus we find

$$Q = Q_{\text{ind}} + Q_{\text{spont}}, \tag{7}$$

where

$$Q_{\text{ind}} = +\frac{2\pi}{\hbar}\sum_{q\gamma}\sum_{p\beta}\sum_{k\alpha}\epsilon_{kp}^{\alpha\beta}w_{kp,q}^{\alpha\beta,\gamma}[f(\epsilon_k^\alpha)-f(\epsilon_p^\beta)]$$
$$\times n_{ph}(\omega_q^\gamma)\delta_{k,p+q}\delta(\epsilon_{kp}^{\alpha\beta}-\omega_q^\gamma), \tag{8a}$$

$$Q_{\text{spont}} = -\frac{2\pi}{\hbar}\sum_{q\gamma}\sum_{p\beta}\sum_{k\alpha}\epsilon_{kp}^{\alpha\beta}w_{kp,q}^{\alpha\beta,\gamma}[f(\epsilon_k^\alpha)-f(\epsilon_p^\beta)]$$
$$\times n_e(\omega_q^\gamma)\delta_{k,p+q}\delta(\epsilon_{kp}^{\alpha\beta}-\omega_q^\gamma). \tag{8b}$$

Here and in the following we assume that the system is in quasiequilibrium where electrons are described by the electron temperature T_e and chemical potential μ, and phonons by the temperature T_{ph}. Thus $f_k^\alpha=f(\epsilon_k^\alpha)$ and $n_q^\gamma=n_{ph}(\omega_q^\gamma)$, where $f(E)=\{\exp[(E-\mu)/k_BT_e]+1\}^{-1}$ is the Fermi function and $n_i(\omega)=[\exp(\omega/kT_i)-1]^{-1}$ the Bose function at tempera-
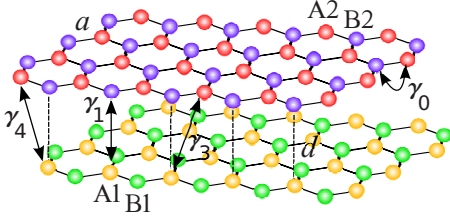
FIG. 1. (Color online) Geometrical structure of bilayer graphene with AB, or Bernal, stacking and the Slonczewski-Weiss-McClure band parameters $\gamma_{0,1,3,4}$. The A1, B1, A2, and B2 atoms of the two sublattices and layers are indicated. The nearest-neighbor distance is $a \approx 0.14$ nm and the interlayer distance is $d \approx 0.37$ nm.

ture T_i. To arrive at form (8b) we have applied $f(\epsilon_k^\alpha)[1-f(\epsilon_p^\beta)]=-[f(\epsilon_k^\alpha)-f(\epsilon_p^\beta)]n_e(\epsilon_{kp}^{\alpha\beta})$.

The only difference between Q_{spont} and Q_{ind} is therefore the sign and the temperature that enters the Bose function. Writing $Q_{\text{ind}}=Q_{\text{ind}}(\mu,T_e,T_{ph})$, we have

$$Q_{\text{spont}}(\mu,T_e) = -Q_{\text{ind}}(\mu,T_e,T_e). \qquad (9)$$

Due to this symmetry, it is only necessary to calculate Q_{ind} explicitly. It is easy to see that the net power transfer is zero if $T_e = T_{ph}$.

Besides the heat current Q, another useful quantity is the linear-response thermal conductance, defined as

$$G(\mu,T) = \frac{\partial}{\partial \Delta T} Q\left(\mu, T + \frac{\Delta T}{2}, T - \frac{\Delta T}{2}\right)\Bigg|_{\Delta T=0}, \qquad (10)$$

where $Q=Q(\mu,T_e,T_{ac})$, $\Delta T=T_e-T_{ac}$, and $T=(T_e+T_{ac})/2$. This is more convenient for characterizing the strength of the electron-phonon coupling because it only depends on a single temperature.

A more physical reason for concentrating on the linear-response regime comes from the assumption of quasiequilibrium. The latter is a commonly used approximation that avoids the need to include the electron-electron collision integral and an equally detailed treatment of the phonon kinetics.[3] Electrons remain in internal equilibrium if the electron-electron interactions are sufficiently strong.[19] (For an example of a case where this is not valid, see Ref. 20.) The same applies to phonons if their relaxation is strong enough, which is typically the case for systems on a substrate. However, although these conditions might not always be satisfied far from equilibrium, we do not expect them to be a serious concern in the linear-response regime.

III. ELECTRONIC STRUCTURE OF MONOLAYER AND BILAYER GRAPHENE

Here we give a very brief reminder on the low-energy band structure of graphene. Figure 1 shows the geometrical structure of BLG. For a tight-binding description we employ the Slonczewski-Weiss-McClure parameters.[12,21–23] In what follows we only use the parameters $\gamma_0 \approx 3$ eV, $\gamma_1 \approx 0.4$ eV and set $\gamma_3 = \gamma_4 = 0$, which is a reasonable approximation at not-too-low energies.[13] MLG is obtained by setting also $\gamma_1 = 0$ and concentrating on one of the layers. The unit cell then

has two atoms and the Hamiltonian for each of the K point of the reciprocal space is a 2×2 matrix, whose eigenvalues give the conical "Dirac" spectrum. In the case of BLG the unit cell has four atoms and thus the low-energy Hamiltonian is a 4×4 matrix. However, using perturbation theory to leading order in $1/\gamma_1$, it may be replaced with an effective 2×2 Hamiltonian in the basis of the "uncoupled" atoms A2 and B1.[12,13,24] The resulting dispersion relation is parabolic.

Using this parabolic-band approximation for BLG, the dispersion relations of the v and c bands and the corresponding eigenstates may be written collectively as

$$\epsilon_k^\alpha = s_\alpha (\hbar v k)^n / \gamma_1^{n-1},$$

$$\phi_k^\alpha = \frac{1}{\sqrt{2}}[1, \pm s_\alpha e^{\pm n i \phi_k}]^T, \qquad (11)$$

where $n=1$ for MLG, $n=2$ for BLG, $s_\alpha = \pm 1$ for $\alpha = c, v$, $\phi_k = \arctan(k_y/k_x)$, $k=|\mathbf{k}|$, and $\hbar v = 3a\gamma_0/2$, with $v \approx 10^6$ m/s. The upper and lower signs correspond to the two different K points (valleys), relative to which the wave vectors $\mathbf{k}$ are counted. The zero of energy is set at the charge neutrality point.

These low-energy results are sufficient for the discussion of interactions of the electrons with acoustic phonons. Atomic-scale scatterers such as short-wavelength optical phonons can also couple the two K points[25,26] but for simplicity we disregard intervalley scattering in our discussion of optical phonons below.

IV. ACOUSTIC PHONONS IN MONOLAYER AND BILAYER GRAPHENE

Long-wavelength acoustic phonons may be treated with continuum theories to a good approximation. An atomistic treatment is required only for optical phonons, see Sec. VI. Here we do not discuss the actual calculation of the phonon modes, which could be described in terms of elasticity theory.[12,17,27]

A. Coupling via deformation potential

The dominant form of electron-phonon coupling for long-wavelength acoustic modes is due to the deformation potential.[17,25,27] For in-plane modes the potential is of the form $D\nabla \cdot \mathbf{u}$, where $\mathbf{u}(\mathbf{r})$ is the displacement vector from elasticity theory and D is the coupling constant, for which values in the range $D=10–50$ eV have been used (Refs. 8, 9, and 27).

The deformation potential is nonzero only for LA modes. Thus we may use the expansion in terms of longitudinal plane waves: $\mathbf{u}(\mathbf{r})=\sum_q u_q \hat{\mathbf{q}} e^{i\mathbf{q}\cdot\mathbf{r}}$. Quantizing this with $u_q = i\sqrt{\hbar^2/(2M\omega_q)}(b_q + b_{-q}^\dagger)$, where $b_q^\dagger$ and b_q are the phonon creation and annihilation operators, the electron-phonon coupling Hamiltonian becomes

$$\hat{H}_{e\text{-}ac} = \sum_{k\alpha,p\beta} \sum_q M_{pk,q}^{\beta\alpha} c_{p\beta}^\dagger c_{k\alpha}(b_q + b_{-q}^\dagger) \qquad (12)$$

with $M_{pk,q}^{\beta\alpha}=-\sqrt{\hbar^2/(2M\omega_q)}Dq\langle p\beta|e^{i\mathbf{q}\cdot\mathbf{r}}|k\alpha\rangle$. Here $\omega_q=\hbar c q$ is the LA phonon dispersion and $M=A\rho$ is the total mass, with

ρ the mass density (of MLG or BLG) and A the area of the system. The wave functions are $\langle r|k\alpha\rangle=e^{ik\cdot r}\phi_k^\alpha/\sqrt{A}$, where Eq. (11) should be used for ϕ_k^α. The coupling constants are then identified from $|M_{pk,q}^{\beta\alpha}|^2=w_{kp,q}^{\alpha\beta}\delta_{p,k+q}$, which yields[10,28]

$$w_{kp,q}^{\alpha\beta}=\frac{\hbar^2}{2M\omega_q}D^2q^2F_{\alpha\beta}(\theta).\tag{13}$$

Here $F_{\alpha\beta}(\theta)=(1+s_\alpha s_\beta\cos n\theta)/2$, $\theta=\phi_p-\phi_k$, and $n=1,2$ for MLG and BLG, respectively.

B. Conservation laws

In scattering of electrons from acoustic phonons, the final wave vectors p allowed by energy and momentum conservation laws (for given initial k) may be determined from the equation $\epsilon_p^\beta=\epsilon_k^\alpha+s\hbar c|p-k|$, where $s=+1$ for absorption and $s=-1$ for emission, and ϵ_k^α and ϵ_p^β are the initial and final energies, respectively. The right-hand side describes a conical surface in momentum-energy space with the apex at (k,ϵ_k^α) and the left-hand side is another surface. In the case of MLG this surface is also a cone while for BLG in the parabolic-band approximation it is a paraboloid. The allowed p values now lie on the p-plane projection of the curve defined by the intersection of the two surfaces. These may be worked out analytically and they are needed for the numerical evaluation of the heat current. However, we skip the details for brevity, see Ref. 29. It is noteworthy that in the case of MLG there cannot be any interband scattering ($\beta\neq\alpha$) when the phonon dispersion is linear[10] while for BLG interband scattering is possible if the initial k is small enough. However, in practice this scattering is strongly suppressed by the coupling constant, Eq. (13).

V. HEAT CURRENT BETWEEN ELECTRONS AND ACOUSTIC PHONONS

Here we use the results of Sec. II for graphene, with the LA phonon coupling constant given by Eq. (13). First we present the general result which can be evaluated numerically and then discuss analytic approximations in the BG and EP limits.

A. Numerical solution

For acoustic LA phonons the most general expression for Q_{ind} without any approximations is

$$Q_{ind}=-\frac{g_eA\hbar D^2}{2(2\pi)^2\rho}\sum_{\alpha\beta}\int_0^\infty dk\,k\int_{q_{min}^{\alpha\beta}}^{q_{max}^{\alpha\beta}}dq\,q^2$$
$$\times\frac{1+s_\alpha s_\beta y(k,q)}{\sqrt{1-[x(k,q)]^2}}|\hbar v_k^\alpha[p(k,q)/k]^{n-2}|^{-1}$$
$$\times n_{ac}(\hbar cq)[f(\epsilon_k^\alpha-\hbar cq)-f(\epsilon_k^\alpha)]\tag{14}$$

with $n=1,2$ as above. Here $v_k^\alpha=s_\alpha n(\hbar v)^n(k/\gamma_1)^{n-1}/\hbar$ is the group velocity and $x(k,q)=-\{[p(k,q)]^2-k^2-q^2\}/(2kq)$ is the cosine of the angle between the incoming k and the phonon q. In the latter $p(k,q)=[s_\alpha s_\beta-s_\beta\hbar cq\gamma_1^{n-1}/(\hbar vk)^n]^{1/n}k$ is the length of $p=k-q$ after imposing conservation laws.
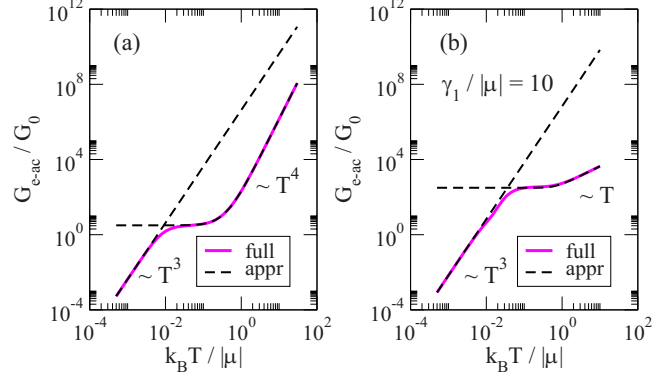

FIG. 2. (Color online) Thermal conductance $G_{e-ac}(\mu,T)$ for (a) MLG and (b) BLG. The unit is $G_0=g_eAD^2\hbar|\mu|^4k_B/[8\pi^2\rho(\hbar v)^6]$ for MLG and $G_0=g_eAD^2\hbar\gamma_1|\mu|^3k_B/[16\pi^2\rho(\hbar v)^6]$ for BLG. The parameters are $c/v=0.02$ and $\gamma_1/|\mu|=10$ in (b). The solid lines (magenta) indicate the full numerical solutions and the dashed lines (black) the analytical approximations.

Moreover, $y(k,q)=n[z(k,q)]^n-n+1$, where $z(k,q)=[k-qx(k,q)]/p(k,q)$ is the cosine of the angle between k and p. Finally, the correct limits $q_{max,min}^{\alpha\beta}$ of the q integral are obtained from the conservation laws, as discussed in Sec. IV B. Using these results together with Eq. (9), the total power Q_{e-ac} may be obtained numerically. An example of the corresponding thermal conductance $G_{e-ac}(\mu,T)$ is represented by the solid lines in Fig. 2.

To obtain analytic estimates, we first expand Eq. (14) to leading order in $c/v\ll1$. In this approximation we may neglect interband transitions ($\beta\neq\alpha$) also for BLG and use $x(k,q)=q/2k$, $p(k,q)=k$, $q_{max}^{\alpha\alpha}=2k$, and $q_{min}^{\alpha\alpha}=0$. In the BG and EP limits the forms of Eqs. (1) and (2) are then recovered. Below we give the results for the coefficients Σ and $g(\mu,T_e)$ for MLG and BLG. The thermal conductances G_{e-ac} obtained from them are shown as the dashed lines in Fig. 2. The agreement with the full numerical solution is very good. The most notable difference between MLG and BLG is the much weaker temperature dependence of G_{e-ac} for $k_BT_e\gg|\mu|$ in BLG.

B. Limits for monolayer graphene

First consider the case of MLG ($n=1$). For a low-temperature approximation of Eq. (14) we may estimate $\epsilon_k^\alpha=s_\alpha\hbar vk\sim\mu$ and $\hbar cq\sim k_BT_{ac}$. If $k_BT_e,k_BT_{ac}\ll2(c/v)|\mu|=k_BT_{BG,MLG}$, we may set $q/2k\to0$ in the q integral and extend the upper limit $q_{max}=2k\to\infty$. Since $\hbar cq\ll|\epsilon_k^\alpha|$, we expand the Fermi function to the first order in $\hbar cq$. The T_e dependence then drops out of Q_{ind} so that the total power takes on the symmetric form of Eq. (1), where $V_d=A$, $\delta=4$, and

$$\Sigma=\frac{\pi^2D^2|\mu|k_B^4}{15\rho\hbar^5v^3c^3}.\tag{15}$$

The same result was derived previously in Ref. 8.

The coupling constant Σ may be expressed in terms of the electron-phonon relaxation rate at the Fermi level and the electronic specific heat.[2] We start from the definition of the

relaxation rate $\tau_{\boldsymbol{k}\alpha}^{-1} = -\partial_{f_{\boldsymbol{k}}^{\alpha}} S_{e\text{-}ph}(f_{\boldsymbol{k}}^{\alpha})|_{f=f_0}$, where $f_0(E) = \{\exp[(E - \mu)/k_B T] + 1\}^{-1}$ and T is the lattice temperature. A similar calculation as for Q_{ind} yields

$$\tau_{k_F}^{-1} = \frac{\pi D^2 k_B^2}{4\rho\hbar^3 v c^3} T^2, \tag{16}$$

where $k_F = |\mu|/(\hbar v)$. (We note that unlike this result, the transport relaxation rate[14,17] is $\propto T^4$.) The electronic specific heat is given by $C = (\pi^2/3)\nu(\mu)k_B^2 T$, where the density of states including the degeneracy $g_e = 4$ is $\nu(E) = 2|E|/(\pi\hbar^2 v^2)$. Identifying $\tau_{k_F}^{-1} = \alpha^* T^2$ and $C = \gamma^* T$, we find $\Sigma = (2/5)\alpha^*\gamma^*$.

Seeking a high-temperature approximation, we require $\hbar c q \ll k_B T_e, k_B T_{ac}$, which allows us to expand also the Bose function. Since for a given k the maximal q is $2k$ and the maximal relevant k is determined by $|\epsilon_k^{\alpha}| \sim \max(|\mu|, k_B T_e)$, the limits translate to $2(c/v)\max(|\mu|, k_B T_e) \ll k_B T_e, k_B T_{ac}$. This is the case considered in Ref. 9 and since $c/v \ll 1$ the limit is equivalent to $T_e, T_{ac} \gg T_{\text{BG,MLG}}$, if $T_e \sim T_{ac}$. In this limit, Q_{ind} depends on both T_e and T_{ac}. Using Eq. (9) then leads to a total power of the asymmetric form in Eq. (2), where $V_d = A$ and

$$g(\mu, T_e) = \frac{D^2 k_B}{30\pi\rho\hbar^5 v^6}[15\mu^4 + 30\pi^2\mu^2(k_B T_e)^2 + 7\pi^4(k_B T_e)^4]. \tag{17}$$

For $k_B T_{\text{BG,MLG}} \ll k_B T_e \ll |\mu|$ this yields $g(\mu, T_e) \propto \mu^4$ and in the limit $|\mu| \ll k_B T_e$ we find $g(\mu, T_e) \propto T_e^4$.

For completeness we mention also the result[14] for the high-temperature relaxation rate in MLG,

$$\tau_{k_F}^{-1} = \frac{D^2 |\mu| k_B}{2\rho\hbar^3 v^2 c^2} T. \tag{18}$$

In this case the relation to $Q_{e\text{-}ac}$ is more complicated than at low temperature.

C. Limits for bilayer graphene

Next consider BLG ($n = 2$). In this case, besides μ, T_e, and T_{ac}, there is an additional energy scale determined by γ_1. In order for the parabolic two-band approximation to be valid, we must require $\max(|\mu|, k_B T_e) \ll \gamma_1$.

To find a low-temperature approximation, we follow similar steps as for MLG. The assumed limit is now $k_B T_e, k_B T_{ac} \ll 2(c/v)\sqrt{\gamma_1|\mu|} = k_B T_{\text{BG,BLG}}$ (with $|\mu| \ll \gamma_1$), using which we find Eq. (1) with $\delta = 4$ but this time

$$\Sigma = \frac{\pi^2 D^2 \gamma_1 k_B^4}{60\rho\hbar^5 v^3 c^3}\sqrt{\frac{\gamma_1}{|\mu|}}. \tag{19}$$

The scaling with temperature is thus similar to the MLG case but the μ dependence is different. Result (19) is valid also in a normal 2D system with effective mass $\gamma_1/(2v^2)$.

For BLG we find the relaxation rate

$$\tau_{k_F}^{-1} = \frac{\pi D^2 k_B^2}{8\rho\hbar^3 v c^3}\sqrt{\frac{\gamma_1}{|\mu|}} T^2, \tag{20}$$

where $k_F = \sqrt{\gamma_1|\mu|}/(\hbar v)$. (The corresponding transport relaxation rate is again $\propto T^4$.) Now the density of states entering C

is approximately $\nu(E) \approx \gamma_1/(\pi\hbar^2 v^2)$. Also in this case the definitions $\tau_{k_F}^{-1} = \alpha^* T^2$ and $C = \gamma^* T$ lead to $\Sigma = (2/5)\alpha^*\gamma^*$.

For BLG the high-temperature (EP) limit $\hbar c q \ll k_B T_e, k_B T_{ac}$ may be written as $2(c/v)\sqrt{\gamma_1 \max(|\mu|, k_B T_e)} \ll k_B T_e, k_B T_{ac}$. This is again equivalent to $T_e, T_{ac} \gg T_{\text{BG,BLG}}$, if additionally $T_e \sim T_{ac} \gg 2(c/v)^2\gamma_1/k_B$. The total power again takes the form of Eq. (2), where now

$$g(\mu, T_e) = \frac{D^2 \gamma_1^3 k_B}{4\pi\rho\hbar^5 v^6}\{2k_B T_e \ln[2\cosh(\mu/2k_B T_e)]\}. \tag{21}$$

In contrast to MLG, if $k_B T_{\text{BG,BLG}} \ll k_B T_e \ll |\mu|$ then $g(\mu, T_e) \propto \mu$ and if $|\mu|$, $2(c/v)\sqrt{\gamma_1 k_B T_e} \ll k_B T_e$ then $g(\mu, T_e) \propto k_B T_e$.

Finally we mention also the BLG result for the high-temperature relaxation rate,

$$\tau_{k_F}^{-1} = \frac{D^2 \gamma_1 k_B}{4\rho\hbar^3 v^2 c^2} T, \tag{22}$$

which is valid in the same limit as assumed above.

VI. OPTICAL PHONONS

For graphene, its multilayers, and graphite the phonon spectra have been studied in detail both experimentally and theoretically.[30–34] In order to describe the crossover from acoustic phonons to optical phonons as the dominating phonon type for heat dissipation, we use some simplified optical-phonon models. For the description of the intrinsic optical modes an atomistic description is needed as a starting point. However, we skip the details here (see Ref. 29), as similar calculations have been reported earlier. Of the intrinsic phonons, we consider explicitly only in-plane LO and TO modes (collectively LT) at long wavelengths, i.e., near the Γ point.[12,27,35–37] (The K-point intrinsic phonons[25] are expected to have coupling constants that differ only by a numerical prefactor.[26]) Additionally, we consider coupling to the "remote" phonons of a dielectric substrate,[15,38,39] which is also a relevant concern for many experiments.[16]

A. Coupling constants for simple phonon models

Let us first consider a model for the long-wavelength in-plane (LT) optical phonons in MLG, for which the LO and TO branches are nearly degenerate, with energy $\Omega_{\text{LT}} \approx 0.2$ eV. In the tight-binding picture of Fig. 1, the strongest coupling to the LT modes comes from the modulation of the nearest-neighbor (A1-B1) coupling amplitude γ_0 (see Ref. 40). The coupling constant is of the form[10]

$$w_{\boldsymbol{kp},\boldsymbol{q}}^{\alpha\beta,\text{LT}} = \frac{9(\gamma_0')^2\hbar^2}{2M\Omega_{\text{LT}}}\frac{1}{2}[1 - s_\alpha s_\beta \cos(\phi_{\boldsymbol{k}} + \phi_{\boldsymbol{p}} - 2\phi_{\hat{\boldsymbol{a}}})], \tag{23}$$

where $M = A\rho_1$, with $\rho_1 \approx 7.6 \times 10^{-7}$ kg/m^2 the mass density of MLG, and $\gamma_0' \approx 40$ eV/nm is the derivative of γ_0 with respect to the nearest-neighbor bond length.[27] The vector $\hat{\boldsymbol{a}}(\boldsymbol{q}) = \hat{\boldsymbol{q}}$ for the LO and $\hat{\boldsymbol{a}}(\boldsymbol{q}) = \hat{\boldsymbol{z}} \times \hat{\boldsymbol{q}}$ for the TO branch, $\hat{\boldsymbol{z}}$ being normal to the plane.

In BLG there are four nearly degenerate LT branches, with $\Omega_{LT} \approx 0.2$ eV since for both LO and TO type modes the atoms in layers 1 and 2 can move either in phase or in opposite phases.[37] With perturbation theory to first order in $\hbar v k / \gamma_1$ we find in this case

$$w_{\boldsymbol{kp},\boldsymbol{q}}^{\alpha\beta,\mathrm{LT}} = \frac{9(\gamma_0')^2 \hbar^2}{2M\Omega_{LT}} \frac{1}{2} \frac{(\hbar v)^2}{\gamma_1^2} \{k^2 + p^2 + 2kp[\pm \cos(\phi_{\boldsymbol{kp}}) \\ - s_\alpha s_\beta \cos(\phi_{\boldsymbol{k\hat{a}}} + \phi_{\boldsymbol{p\hat{a}}})] \mp s_\alpha s_\beta [k^2 \cos(2\phi_{\boldsymbol{p\hat{a}}}) \\ + p^2 \cos(2\phi_{\boldsymbol{k\hat{a}}})]\}, \tag{24}$$

where $M = A\rho_2$, $\rho_2 = 2\rho_1$, and $\phi_{\boldsymbol{kp}} = \phi_{\boldsymbol{k}} - \phi_{\boldsymbol{p}}$. The upper and lower signs are for the in-phase and opposite-phase modes, respectively. For BLG there are also the out-of-plane optical modes with energy $\Omega_{ZO} \approx 0.1$ eV which could couple linearly to electrons via the modulation of the A1-B2 bond and thus γ_1 but we estimate them to be relatively unimportant for the energy relaxation (see Ref. [41]).

Finally, in addition to these intrinsic phonons, we consider possibility of coupling to remote surface phonons of a dielectric substrate.[15,16,39] The coupling is due to the electric polarization associated with the phonons, which modulates the scalar potential on the graphene. For simplicity we again disregard the possibility of intervalley scattering.[15] The coupling constant is given by[15,38]

$$w_{\boldsymbol{kp},\boldsymbol{q}}^{\alpha\beta,\mathrm{rem}} = \beta_{\mathrm{rem}} \frac{e^2 \Omega_{\mathrm{rem}}}{2\varepsilon_0 A} \frac{1}{q} e^{-2qz} F_{\alpha\beta}(\theta), \tag{25}$$

where Ω_{rem} is the energy of the relevant surface mode, $z \geq 0$ is the effective distance between the graphene and the substrate, $F_{\alpha\beta}(\theta)$ is as in Eq. (13), and ε_0 is the permittivity of vacuum in SI units. If there is only a single relevant surface mode, $\beta_{\mathrm{rem}} = (\varepsilon_s - \varepsilon_\infty)/[(\varepsilon_s + 1)(\varepsilon_i + 1)]$, where ε_s and ε_∞ are the static and high-frequency dielectric constants of the insulator.[38] If there are several surface modes, Eq. (25) should be additionally weighted by the corresponding relative oscillator strengths.[15]

B. Heat current between electrons and optical phonons

When the momentum conservation is imposed, $q = \sqrt{k^2 + p^2 - 2kp \cos\theta}$, where $\theta = \phi_{\boldsymbol{k}} - \phi_{\boldsymbol{p}}$. All the coupling constants may then be expressed in terms of only k, p, and $\cos\theta$. For an electron dispersion of the form $\epsilon_k^\alpha = s_\alpha \epsilon_k$, $\epsilon_k > 0$, the heat current between electrons and dispersionless optical phonons may be written

$$Q_{e\text{-}op}^{(\gamma)} = A q_{e\text{-}op}^{(\gamma)}(\mu, T_e)[n_e(\Omega_\gamma) - n_{ph}(\Omega_\gamma)], \tag{26}$$

where (including degeneracy of $g_e = 4$)

$$q_{e\text{-}op}^{(\gamma)} = \frac{A}{4\hbar} \sum_\gamma \Omega_\gamma^2 \int_{-\infty}^{\infty} \nu(\Omega_\gamma x) \nu[\Omega_\gamma(x-1)] \\ \times \int_{-\pi}^{\pi} d\theta w^{\alpha\beta,\gamma}[k(\Omega_\gamma|x|), k(\Omega_\gamma|x-1|), \cos\theta] \\ \times \{f[\Omega_\gamma(x-1)] - f(\Omega_\gamma x)\} dx. \tag{27}$$

Here $\alpha\beta$ are chosen such that $s_\alpha = \mathrm{sign}(x)$ and $s_\beta = \mathrm{sign}(x - 1)$, $\nu(\epsilon)$ is the density of electronic states, and $k(\epsilon)$ the inverse of ϵ_k. The interval $0 < x < 1$ corresponds to interband scattering.

In the case of the LT modes further simplification is achieved by summing over the degenerate LT modes γ. The angle-dependent terms of the coupling constants [Eq. (23)] or [Eq. (24)] then cancel and the angle integral in Eq. (27) becomes trivial. Thus for MLG (Ref. [9])

$$q_{e\text{-}op}^{(\mathrm{LT})}(\mu, T_e) = \frac{9\Omega^3(\gamma_0')^2 \hbar}{\pi(\hbar v)^4 \rho_1} \mathcal{F}(\mu, T_e), \tag{28}$$

where the factor $g_e = 4$ is included, $\Omega = \Omega_{LT}$, and

$$\mathcal{F}(\mu, T_e) = \int_{-\infty}^{\infty} |x(1-x)|\{f[\Omega(x-1)] - f(\Omega x)\} dx. \tag{29}$$

For $k_B T_e \ll \Omega$, $\mathcal{F}(0, T_e) \approx 1/6$. Similarly for BLG

$$q_{e\text{-}op}^{(\mathrm{LT})}(\mu, T_e) = \frac{18\Omega^3(\gamma_0')^2 \hbar}{\pi(\hbar v)^4 \rho_2} \frac{\gamma_1}{\Omega} \mathcal{G}(\mu, T_e), \tag{30}$$

where

$$\mathcal{G}(\mu, T_e) = \int_{-\infty}^{\infty} \frac{1}{4}(|x| + |x-1|)\{f[\Omega(x-1)] - f(\Omega x)\} dx. \tag{31}$$

For $k_B T_e \ll \Omega$, $\mathcal{G}(0, T_e) \approx 1/4$. We note that due to the assumed parabolic dispersion, this result is a good approximation only close to $|\mu| = 0$. For the case of the remote phonons, the angle integral in Eq. (27) is quite complicated but in the limit $z \to 0$ it may be carried out analytically for both MLG and BLG. However, the expressions are complicated and we skip them here.

The numerical results for the prefactors $q_{e\text{-}op}^{(\gamma)}$ are shown in Fig. 3. For the remote phonons we use $z = 0$ and the values for 6H-SiC (see Ref. [42]), where $\varepsilon_s = 9.72$, $\varepsilon_\infty = 6.52$, $\Omega_{\mathrm{rem}} = 116$ meV, and hence $\beta_{\mathrm{rem}} = 0.040$. It is seen from Fig. 3 that the prefactors for the remote phonons are considerably higher than those of the intrinsic phonons. This fact combined with $\Omega_{\mathrm{rem}} < \Omega_{LT}$ means that for heat dissipation the remote phonons may in practice always be the more important ones. The limit $z = 0$ overestimates the coupling constant somewhat, but $q_{e\text{-}op}^{(\mathrm{rem})}$ decays with distance at most proportionally to $e^{-2q_{\max}z}$, where, for example, for MLG at $k_B T_e \ll \Omega_{\mathrm{rem}}$ we find $q_{\max} = (\Omega_{\mathrm{rem}} + 2|\mu|)/(\hbar v)$ and thus $q_{\max}^{-1} \approx 6.2$ nm when $\mu = 0$. The use of SiO_2 would reduce $\varepsilon_s - \varepsilon_\infty$ but then one of the two modes with appreciable oscillator strengths also has a lower energy.[39] The corresponding crossover temperatures between $Q_{e\text{-}ac}$ and $Q_{e\text{-}op}$ are discussed below.

VII. DISCUSSION AND CONCLUSIONS

Let us briefly discuss the implications of our results. A common experimental situation where the heating of electrons occurs is that of a two-probe measurement with a finite bias voltage V. The Joule heat created at some point of the
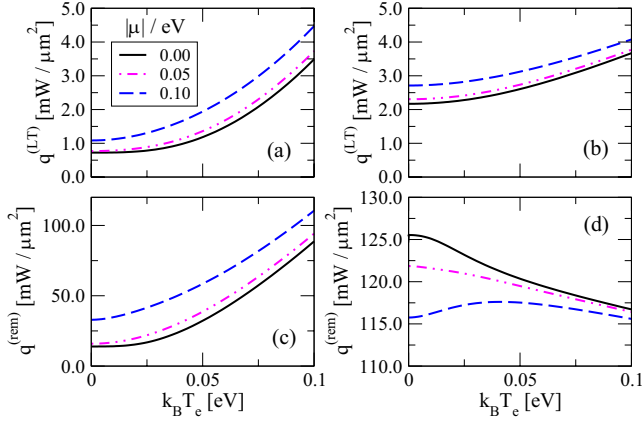
FIG. 3. (Color online) Prefactors $q_{e\text{-}op}^{(\text{LT})}$ and $q_{e\text{-}op}^{(\text{rem})}$ of the electron-optical-phonon heat currents for different doping levels. (a) and (c) are for MLG, and (b) and (d) for BLG. Upper panels are for the intrinsic LT phonons and the lower ones for the remote phonons, with $z=0$.

system is dissipated from the electrons in basically two ways, either by a transfer to phonons or by diffusion of the electrons away from the heated region (e.g., into the electrodes). The static situation is described by a heat-balance equation $\nabla \cdot \boldsymbol{j}_Q + P_{e\text{-}ac} = P_J$, where $\boldsymbol{j}_Q$ is the heat current density while $P_{e\text{-}ac}$ and P_J are the local electron-acoustic-phonon power and Joule power per area, respectively. We assume for simplicity that the Wiedemann-Franz law applies (see Ref. 43) so that $\boldsymbol{j}_Q = -\kappa \nabla T_e$, where $\kappa = \mathcal{L}\sigma T_e$ is the heat conductivity, σ is the electrical conductivity and $\mathcal{L} = (\pi^2/3)(k_B/e)^2$ is the Lorenz number. To find some order-of-magnitude estimates, we assume a quasi-one-dimensional situation with a sample of length L and consider the simpler, discretized equation $P_{\text{diff}} + P_{e\text{-}ac} = P_J$ with the diffusion power $P_{\text{diff}} = (4\mathcal{L}\sigma/L^2)(T^2 - T_0^2)$ and Joule power $P_J = \sigma V^2/L^2$. We also concentrate on the low-temperature regime, $k_B T \ll k_B T_{\text{BG,MLG}} = 2(c/v)|\mu|$ for MLG and $k_B T \ll k_B T_{\text{BG,BLG}} = 2(c/v)\sqrt{\gamma_1|\mu|}$ for BLG so that $P_{e\text{-}ac}$ is of the form $P_{e\text{-}ac} = \Sigma(T^4 - T_0^4)$. Here T is the electron temperature in the middle of the graphene sample and we assume the acoustic phonons and the electrons in the leads to remain at the bath temperature T_0.

Clearly, at low enough T_0 and bias V the diffusion power dominates over the phonon power ($P_{e\text{-}ac} < P_{\text{diff}}$). However, with increasing T_0 or V there is a crossover to an electron-phonon dominated regime ($P_{e\text{-}ac} > P_{\text{diff}}$). If $T_0 > T_{0x} = 2\mathcal{L}\sigma/(\Sigma L^2)$ then $P_{e\text{-}ac}$ dominates also in the linear-response regime (arbitrarily small V and $\Delta T = T - T_0$). For $T_0 < T_{0x}$ there is a finite crossover voltage $V_{\text{cr}} = \sqrt{8\mathcal{L}(T_{\text{cr}}^2 - T_0^2)}$, with the corresponding temperature $T_{\text{cr}} = \sqrt{4\mathcal{L}\sigma/(\Sigma L^2) - T_0^2}$.

When the phonon power dominates, $P_{e\text{-}ac} \approx P_J$. Since P_J can be deduced from the current-voltage characteristics, measurement of the electron temperature in the presence of heating can also act as an indirect measurement of the electron-phonon coupling constant. To see if this regime can be reached before the low-temperature approximation for $P_{e\text{-}ac}$ breaks down, we estimate the crossover temperatures. Using $D = 30$ eV we find for MLG,
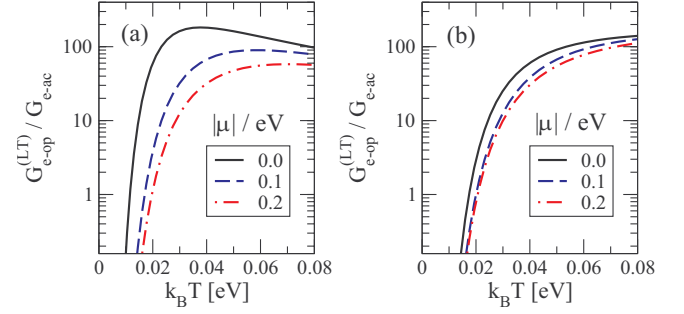

FIG. 4. (Color online) The ratio of (LT) optical-phonon thermal conductance $G_{e\text{-}op}^{(\text{LT})}(\mu, T)$ and that of acoustic phonons $G_{e\text{-}ac}(\mu, T)$ for (a) MLG and (b) BLG. The parameters are $D = 30$ eV and $|\gamma_0'| = 40$ eV/nm (Ref. 27). In both cases the crossover point $G_{e\text{-}op}^{(\text{LT})}/G_{e\text{-}ac} = 1$ moves to higher temperature with increasing $|\mu|$.

$$T_{0x} = 5 \text{ K} \times \frac{(\sigma/\sigma_0)^{1/2}}{(L/1 \ \mu\text{m})(|\mu|/0.3 \text{ eV})^{1/2}} \tag{32}$$

and for BLG,

$$T_{0x} = 11 \text{ K} \times \frac{(\sigma/\sigma_0)^{1/2}(|\mu|/0.3 \text{ eV})^{1/4}}{(L/1 \ \mu\text{m})}, \tag{33}$$

where $\sigma_0 = 4e^2/h$. These are only valid if $T_{0x} \ll T_{\text{BG,MLG/BLG}}$. We find $T_{\text{BG,MLG}} = 140 \text{ K} \times (|\mu|/0.3 \text{ eV})$ and $T_{\text{BG,BLG}} = 160 \text{ K} \times (|\mu|/0.3 \text{ eV})^{1/2}$. Since the electron-phonon interaction becomes more important for increasing L, it seems possible to meet these criteria with long enough samples.

The estimate could be improved by taking into account that σ also grows with μ differently for MLG and BLG, and it may also depend on temperature.[44,45] However, these details depend on the types of scattering. In practice, the dominant form of scattering in graphene on a substrate is from impurities.[46,47] Experiments indicate that σ grows roughly linearly with charge density,[48] which yields $\sigma \sim \mu^2$ for MLG and $\sigma \sim \mu$ for BLG. We also note that the diffusion power can be reduced or even eliminated by the use of superconducting leads.

At high enough temperature there is another crossover, where optical phonons begin to dominate the electron-phonon heat transfer.[9,10] Although the conductance $G_{e\text{-}op}$ is exponentially suppressed at low temperature, $G_{e\text{-}ac}$ is also small and for MLG quite strongly temperature dependent, with $G_{e\text{-}ac} \sim T^4$ at $\mu = 0$. This can lead to surprisingly low crossover temperatures. Here we consider explicitly only the intrinsic LT optical-phonon modes. Figure 4 shows the ratios $G_{e\text{-}op}^{(\text{LT})}/G_{e\text{-}ac}$ of optical and acoustic-phonon thermal conductances for MLG and BLG. As found previously,[9,10] optical phonons can become dominant already well below room temperature (150 K for MLG and 200 K for BLG) and the crossover moves to higher temperatures with increasing carrier density. The nonmonotonous behavior[9] of $G_{e\text{-}op}^{(\text{LT})}/G_{e\text{-}ac}$ in the case of MLG is not present in BLG. As found above, if the graphene is on a dielectric substrate, the dominant optical modes are most likely the surface modes of the dielectric.[15,16] By using the parameter values quoted in Sec. VI B for SiC and studying $G_{e\text{-}op}^{(\text{rem})}/G_{e\text{-}ac}$ as in Fig. 4, we

find crossover temperatures 60 K for MLG and 80 K for BLG at $\mu=0$. For SiO_2, using the parameters quoted in Ref. 15, the results are as low as 30 K and 50 K, respectively.

We note that the above results depend on the poorly known parameters D and γ_0' in their second powers while c and v also appear with high powers. This makes quantitative predictions difficult and increases the need for an experimental determination of the coupling constants. Finally it should also be noted that if the bias voltage exceeds the value $\sim\Omega_{LT}/e=0.2$ V, scattering from optical phonons becomes very important also at low bath temperature.[16,49,50] In this case the optical phonons can have a highly nonequilibrium distribution.[51–53]

To conclude, we have calculated the power transfer between the electron and phonon systems in monolayer and bilayer graphene, assuming the existence of quasiequilibrium. In particular, we have studied the coupling to longitudinal-acoustic phonons and different types of optical phonons. For the former we have calculated the power numerically and derived analytic expressions in low- and high-temperature limits. The power transfer to acoustic phonons dominates the diffusion power above a certain crossover temperature, estimated in Eqs. (32) and (33). At even higher temperatures, there is another crossover where optical phonons begin to dominate and we have estimated also these crossover temperatures numerically (Fig. 4). We find that for graphene on the substrate the most relevant optical phonons are likely to be the surface optical modes of the substrate.

[1] P. B. Allen, Phys. Rev. Lett. **59**, 1460 (1987).

[2] F. C. Wellstood, C. Urbina, and J. Clarke, Phys. Rev. B **49**, 5942 (1994).

[3] F. Giazotto, T. T. Heikkilä, A. Luukanen, A. M. Savin, and J. P. Pekola, Rev. Mod. Phys. **78**, 217 (2006).

[4] F. W. J. Hekking, A. O. Niskanen, and J. P. Pekola, Phys. Rev. B **77**, 033401 (2008).

[5] G. D. Mahan, *Many-Particle Physics*, 3rd ed. (Kluwer Academic/Plenum, New York, 2000).

[6] A. Sergeev and V. Mitin, Phys. Rev. B **61**, 6041 (2000).

[7] J. T. Karvonen, L. J. Taskinen, and I. J. Maasilta, Phys. Rev. B **72**, 012302 (2005).

[8] S. S. Kubakaddi, Phys. Rev. B **79**, 075417 (2009).

[9] R. Bistritzer and A. H. MacDonald, Phys. Rev. Lett. **102**, 206410 (2009).

[10] W.-K. Tse and S. Das Sarma, Phys. Rev. B **79**, 235406 (2009).

[11] K. S. Novoselov, A. K. Geim, S. V. Morozov, D. Jiang, Y. Zhang, S. V. Dubonos, I. V. Grigorieva, and A. A. Firsov, Science **306**, 666 (2004).

[12] A. H. Castro Neto, F. Guinea, N. M. R. Peres, K. S. Novoselov, and A. K. Geim, Rev. Mod. Phys. **81**, 109 (2009).

[13] E. McCann and V. I. Fal'ko, Phys. Rev. Lett. **96**, 086805 (2006).

[14] E. H. Hwang and S. Das Sarma, Phys. Rev. B **77**, 115449 (2008).

[15] S. Fratini and F. Guinea, Phys. Rev. B **77**, 195415 (2008).

[16] I. Meric, M. Y. Han, A. F. Young, B. Ozyilmaz, P. Kim, and K. L. Shepard, Nat. Nanotechnol. **3**, 654 (2008).

[17] E. Mariani and F. von Oppen, Phys. Rev. Lett. **100**, 076801 (2008); **100**, 249901(E) (2008).

[18] Z. Chen, W. Jang, W. Bao, C. N. Lau, and C. Dames, Appl. Phys. Lett. **95**, 161910 (2009).

[19] R. Bistritzer and A. H. MacDonald, Phys. Rev. B **80**, 085109 (2009).

[20] V. V. Kabanov and A. S. Alexandrov, Phys. Rev. B **78**, 174514 (2008).

[21] J. C. Slonczewski and P. R. Weiss, Phys. Rev. **109**, 272 (1958).

[22] J. W. McClure, Phys. Rev. **108**, 612 (1957).

[23] M. S. Dresselhaus and G. Dresselhaus, Adv. Phys. **51**, 1 (2002).

[24] J. Nilsson, A. H. Castro Neto, F. Guinea, and N. M. R. Peres, Phys. Rev. B **78**, 045405 (2008).

[25] H. Suzuura and T. Ando, J. Phys. Soc. Jpn. **77**, 044703 (2008).

[26] F. Rana, P. A. George, J. H. Strait, J. Dawlaty, S. Shivaraman, M. Chandrashekhar, and M. G. Spencer, Phys. Rev. B **79**, 115447 (2009).

[27] H. Suzuura and T. Ando, Phys. Rev. B **65**, 235412 (2002).

[28] S. V. Rotkin, V. Perebeinos, A. G. Petrov, and P. Avouris, Nano Lett. **9**, 1850 (2009).

[29] J. Viljas and T. Heikkilä, arXiv:1002.3502 (unpublished).

[30] M. Mohr, J. Maultzsch, E. Dobardžić, S. Reich, I. Milošević, M. Damnjanović, A. Bosak, M. Krisch, and C. Thomsen, Phys. Rev. B **76**, 035439 (2007).

[31] J.-A. Yan, W. Y. Ruan, and M. Y. Chou, Phys. Rev. B **77**, 125401 (2008).

[32] K. H. Michel and B. Verberck, Phys. Rev. B **78**, 085424 (2008).

[33] L. M. Malard, M. H. D. Guimarães, D. L. Mafra, M. S. C. Mazzoni, and A. Jorio, Phys. Rev. B **79**, 125426 (2009).

[34] S. Viola Kusminskiy, D. K. Campbell, and A. H. Castro Neto, Phys. Rev. B **80**, 035401 (2009).

[35] T. Ando, J. Phys. Soc. Jpn. **74**, 777 (2005).

[36] W.-K. Tse and S. Das Sarma, Phys. Rev. Lett. **99**, 236802 (2007).

[37] T. Ando and M. Koshino, J. Phys. Soc. Jpn. **78**, 034709 (2009).

[38] S. Q. Wang and G. D. Mahan, Phys. Rev. B **6**, 4517 (1972).

[39] M. V. Fischetti, D. A. Neumayer, and E. A. Cartier, J. Appl. Phys. **90**, 4587 (2001).

[40] Unlike acoustic phonons or the remote optical phonons of a substrate, the intrinsic optical modes modulate the onsite energies only weakly. We have checked this with the tight-binding parametrization of D. A. Papaconstantopoulos and M. J. Mehl, J. Phys.: Condens. Matter **15**, R413 (2003) which yields onsite shifts roughly an order of magnitude smaller than those of the hopping integrals for a perturbation corresponding to a Γ point LO/TO mode.

[41] By modeling the out-of-plane optical modes of bilayer as a mode where the A1 and B2 atoms move in opposite phases, thus modulating γ_1 (i.e., the effective mass), we find a coupling constant of the form $w_{kp,q}^{\alpha\beta,\text{ZO}} = [2(\gamma_1')^2\hbar^2/(M\Omega_{\text{ZO}})]\delta_{\alpha\beta}(\hbar v/\gamma_1)^2 kp$. Here $M = A\rho_2$ and γ_1' is the derivative of γ_1 with respect to the A1-B2 bond length. Since there is no interband coupling, such a mode is relatively ineffective at dissipating energy for $|\mu|, k_B T_e \ll \Omega_{\text{ZO}}$.

[42] H. Nienhaus, T. U. Kampen, and W. Mönch, Surf. Sci. **324**, L328 (1995).

[43] M. Trushin and J. Schliemann, Phys. Rev. Lett. **99**, 216602 (2007).

[44] K. I. Bolotin, K. J. Sikes, J. Hone, H. L. Stormer, and P. Kim, Phys. Rev. Lett. **101**, 096802 (2008).

[45] M. Müller, M. Bräuninger, and B. Trauzettel, Phys. Rev. Lett. **103**, 196801 (2009).

[46] S. Adam and S. Das Sarma, Phys. Rev. B **77**, 115436 (2008).

[47] S. Das Sarma, E. Hwang, and E. Rossi, Phys. Rev. B **81**, 161407 (2010).

[48] S. V. Morozov, K. S. Novoselov, M. I. Katsnelson, F. Schedin, D. C. Elias, J. A. Jaszczak, and A. K. Geim, Phys. Rev. Lett. **100**, 016602 (2008).

[49] A. Barreiro, M. Lazzeri, J. Moser, F. Mauri, and A. Bachtold, Phys. Rev. Lett. **103**, 076601 (2009).

[50] J. Chauhan and J. Guo, Appl. Phys. Lett. **95**, 023120 (2009).

[51] C. Auer, F. Schürrer, and C. Ertler, Phys. Rev. B **74**, 165409 (2006).

[52] M. Lazzeri and F. Mauri, Phys. Rev. B **73**, 165419 (2006).

[53] D. Song, F. Wang, G. Dukovic, M. Zheng, E. D. Semke, L. E. Brus, and T. F. Heinz, Phys. Rev. Lett. **100**, 225503 (2008).